Heliyon 9 (2023) e18158

Contents lists available at ScienceDirect

Heliyon

journal homepage: www.cell.com/heliyon

Early-phase rotator training impairs tissue repair and functional recovery after spinal cord injury

Junhao Deng [a,b,1], Fanqi Meng [c,1], Jianpeng Gao [a,1], Kexue Zhang [d], Zhongyang Liu [a], Ming Li [a], Xiao Liu [a], Jiantao Li [a], Yu Wang [e], Licheng Zhang [a,b,*], Peifu Tang [a,b]

[a] Department of Orthopedics, The Chinese PLA General Hospital, Beijing, 100853, China
[b] School of Life Sciences, Tsinghua University, Beijing, 100084, China
[c] Department of Anesthesiology, Xuanwu Hospital Capital Medical University, Beijing, 100050, China
[d] Department of Pediatric Surgery, The Chinese PLA General Hospital, Beijing, 100853, China
[e] Beijing Key Lab of Regenerative Medicine in Orthopaedics, Key Laboratory of Musculoskeletal Trauma and War Injuries PLA, Institue of Orthopaedics, The Chinese PLA General Hospital, Beijing, 100853, China

ARTICLE INFO

Keywords:
Spinal cord injury
Rotarod training
Rehabilitative training
Inflammation
Early-phase training

ABSTRACT

Spinal cord injury (SCI) is a devastating disorder that often results in severe sensorimotor function impairment with limited recovery of function. In recent years, rehabilitation training for spinal cord injury has gradually emerged, and some of them play an important role in the repair of spinal cord injury However, the optimal training regimen for SCI remains to be determined. In this study, we explore the effects of rotarod training (began at 7 days post-injury) on the recovery of motor function after SCI, as well as its possible repair mechanism from the aspects of function and histopathological changes, the behaviors of specific trophic factors and cytokines, and the expression profile of specific genes. Multiple functional assessments showed that rotarod training initiated at 7 days post-injury is unsuitable for promoting neuro-electrophysiological improvement and trunk stability, but impaired functional coordination and motor recovery. In addition, rotarod training has negative effects on spinal cord repair after SCI, which is manifested as an increase of lesion area, a decrease in neuronal viability, a deterioration in immunomicroenvironment and remyelination, a significant reduction in the expression of trophic factors and an increase in the expression of pro-inflammatory factors. RNA sequencing suggested that the genes associated with angiogenesis and synaptogenesis were significantly downregulated and the PI3K-AKT pathway was inhibited, which was detrimental to spinal cord repair and impeded nerve regeneration. These results indicate that immediate rotarod training after SCI is currently unsuitable for rehabilitation in mice.

1. Introduction

Spinal cord injury (SCI) is a devastating disorder with approximately 3 million SCI patients worldwide and 180,000 new cases reported every year [1], which often causes severe and permanent motor and sensory function impairments in patients with SCI [2,3]. Persisting functional deficits would inevitably affect overall health and impose a high psychological and financial burden on

* Corresponding author. Department of Orthopedics, The Chinese PLA General Hospital, Beijing, 100853, China
E-mail address: zhanglcheng301@163.com (L. Zhang).
[1] These author contributed equally to This work and should be considered the co-first authors.

https://doi.org/10.1016/j.heliyon.2023.e18158
Received 14 January 2023; Received in revised form 27 May 2023; Accepted 10 July 2023
Available online 12 July 2023

individuals with SCI. Unfortunately, no effective treatment for SCI is currently available due to the elusive and complex pathophysiologic mechanism after SCI [4,5]. Thus, the exploration of disease-modifying therapy for SCI is a high priority.

Over the past decades, we have witnessed a flourishing of different strategies for spinal cord repair after SCI. Among these novel approaches, repeated physical training, like treadmill training, gait training, walk training, and swimming have shown great potential for functional recovery following SCI [6–8], as exercise might be able to provide motor practice of paralyzed limbs as well as sensory inputs into the injured spinal cord after SCI although the underlying mechanism remains poorly understood [5]. However, the training contributed to fairly limited function improvement in the complete SCI models [9,10], whereas the training also produced conflicting outcomes of functional recovery in the incomplete SCI models [11,12]. On the other hand, different kinds of training promoted functional improvement in varying degrees [13–15], implying that the most appropriate type of training remains to be determined [16].

Rotarod training is a type of forced active exercise that is often used for the promotion of locomotive coordination, balance, and

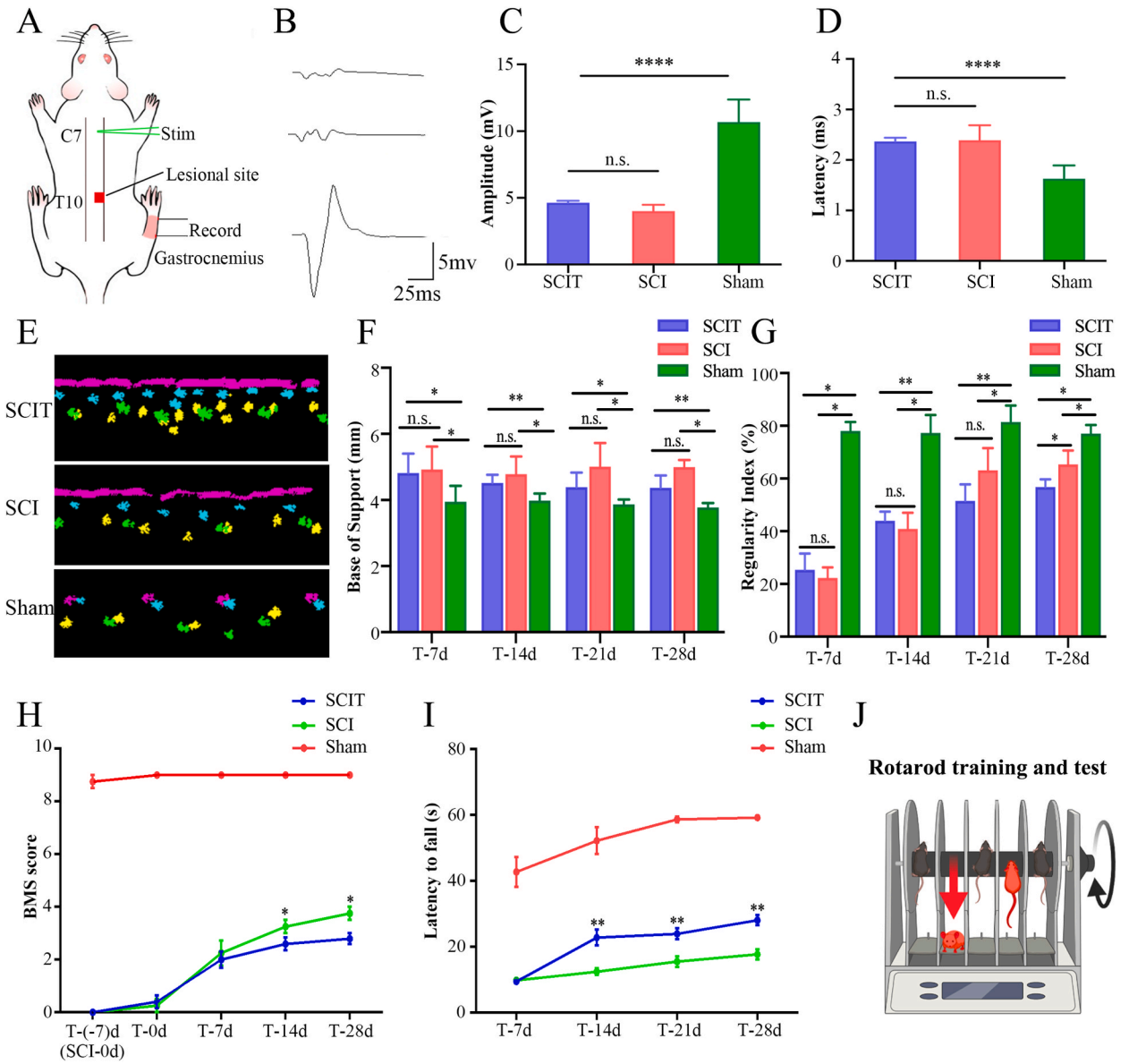

Fig. 1. The functional recovery assessment following rotarod training. **A, B** The process of electrophysiological evaluation (A), and the representative recording of action potentials in SCIT, SCI, and Sham group (B, upper-middle-bottom). **C, D** The amplitude and latency were measured. No significant difference was detected in SCIT and SCI groups (n = 6 in each group). E-**G** The gait analysis by Catwalk XT. The representative footprints were displayed in (E), and the base of support and regularity index were also calculated in (F) and (G), respectively (n = 6 in each group, two-way ANOVA analysis). **H, I** The BMS and rotarod test were evaluated at multiple time points in three groups (n = 6 in each group). **J** The scheme of rotarod training regimen and rotarod test. *, **, **** and n.s. indicate $P < 0.05$, $P < 0.01$, $P < 0.0001$, and no statistical difference, respectively.

anti-fatigue performance [17,18]. When rodent animals were put on the rotarod bar, they had to continuously run and maintain the balance to avoid falling from the rotating bar, for which they received intensive active training. In 2008, Cendelín et al. [19] reported that rotarod training could potentiate the spatial learning ability after a session of training in olivocerebellar degenerated mice. Recently, Nakagawa et al. [17] found that rotarod training led to a significant functional recovery via promoting the axonal remodeling of the corticospinal tract following traumatic brain injury in mice. Nevertheless, there are few studies evaluating rotarod training as an effective treatment for mice with SCI at present.

Therefore, the object of the current study was to explore the effects of rotarod training on locomotion recovery as well as its potential mechanism for spinal cord repair after SCI focusing on the changes of function, histopathology, the behaviors of particular trophic factors and cytokines, and the profile of specific genes expression (Sup. Fig. 1).

2. Materials and methods

2.1. Animals

Age-matched wild-type C57BL/6J mice of both genders were used in this study (5–6 weeks old; purchased from SPF Biotechnology Co., Ltd, Beijing). Mice were group housed under a 12 h light/dark cycle with free access to food and water in the animal center of Chinese PLA General Hospital. In this study, 120 mice were randomly assigned to three groups: Sham group, SCI with rotarod training group (SCIT group), and SCI with no training group (SCI group), and 40 mice for each group. All experiments were approved by the animal ethics committee of the Chinese PLA General Hospital (Approval No. SQ2020039) and performed in strict accordance with the guidelines for the care and use of laboratory animals from the National Institute of Health.

2.2. Spinal cord injury procedures

The spinal cord hemisection procedure at the lower thoracic level was performed as previously described [2,20]. Briefly, all mice were placed on a heating panel at 37 °C and anesthetized intraperitoneally with sodium pentobarbital (10.0 ml/kg body weight in 0.9% NaCl). Once properly anesthetized, the dorsal surface of each mouse was shaved and disinfected with iodophor twice. Then mice would receive a dorsal laminectomy at the T9-11 segment of the spinal cord to expose the corresponding area, and a right-lateral hemisection was made at T9-10 spinal cord level with an ophthalmic side cutting scalpel (Caliber ophthalmic, PA, USA). Tension in the right limb was immediately abolished, indicating that the model had been successfully established. In the Sham group, the spinal cord was only exposed but not injured. After spinal cord injury, muscle and skin above this segment were carefully sutured in layers, and erythromycin was applied to prevent infection. Mice were placed on another heating panel until they recovered from anesthesia and then returned to the clean home cage. Animals were closely monitored for the next 24 h during recovery. Bladders of SCI mice were expressed manually twice a day until the spinal cord-to-bladder micturition reflex developed (8–12 days).

2.3. Rotarod training and rotarod test

Before the SCI procedure, mice in all groups received rotarod training at the lowest rotation speed for 5 min per day in a row of seven days to accustom further rotarod tests and training.

In the SCIT group, the rotarod training was conducted with Mouse Rota-Rod (B&E TEKSYSTEMS LTD, Beijing, China) beginning 7 days after injury. Each mouse was trained to stay on the rotating rod for 5 min with an accelerating speed of 4–40 rpm, Each mouse received 6 trials per day (5 min per trial) in a row of five consecutive days a week. The training was conducted for four weeks.

Mice in three groups underwent rotarod assessment the next day after the training session as previously stated [17]. For the locomotion analysis, mice were put on the rotating drum and the rotation speed also accelerated smoothly from 4 to 40 rpm over 5 min. The time length was recorded when mice fell off. If the mice did not fall off in 1 min, the mice reached the maximum trial time. Each mouse would be tested 5 times in a session.

2.4. Basso mouse scale (BMS) score

The locomotion of the hindlimb was evaluated by the BMS score as stated before (Table 2) [21]. The BMS score is a 9-point rating scale with normal locomotion scoring 9 and complete paralysis scoring 0. Mice received BMS tests at −7, 0, 7, 14, and 28 days after injury by two investigators who were blinded to this study.

2.5. Catwalk XT gait analysis

Mice ($n = 6$ in each group) gaits were analyzed at 1, 2, 3, and 4 weeks immediately following rotarod training with a video-based analysis system, Catwalk XT (Noldus, Wageningen, Netherlands.) [22]. Each mouse was put on the illuminated glass wall and allowed to walk forward. Real-time movie images and footprints were captured when toes contacted the stepping floor. Based on the toe position, gesture, pressure, and touched area, parameters such as the base of support (BS) and regularity index (RI) were calculated and compared between different groups. BS, a measure of trunk stability, was the distance from feet to hindlimb perpendicular to the standing position. The lower value of BS indicates the better stability of the mouse trunk. RI, a sign of body coordination, refers to the ratio of real coordination to the normal one of mouse limbs. RI could be calculated by the paw placement (PP) and normal step

sequence pattern (NSSP) via this formula: RI= (NSSP × 4)/PP × 100% [23]. Generally, the bigger the RI, the better the coordination of the mouse body and the less the wrong gait sequence.

2.6. Electrophysiological analyses

Animal electrical activity was evaluated at 5 weeks post-injury as previously described [2,24]. Briefly, after proper anesthesia, each mouse received laminectomy to re-expose the spinal cord at T9-T10 (n = 3 mice in each group). Then, the electrophysiological experiment was performed using the electromyography machine (Medtronic, Minneapolis, MN, USA). The bi-polar stimulating electrode was placed on the C7 or T1 spinal segment and one unipolar recording electrode was put on the gastrocnemius muscle to record the compound muscle action potentials (CMAP) after electrical stimulation (intensity: 3.00 mA, frequency: 10 Hz). The ground electrode was put into the subcutaneous tissue. The peak amplitude and latency of each CMAP were recorded to compare the recovery of nerve conduction function among the three groups.

2.7. Histological procedures

2.7.1. Haematotoxylin and eosin (HE) staining and measuring the lesion area

HE staining was performed according to manufacturer protocol [25]. In brief, after well deparaffinization and rehydration, tissue sections from the T10 segment of the spinal cord were incubated with Haematoxylin (G1120, Solarbio, China) for 5 min followed by 3 min in Differentiation solution and then rinsed in distilled water. Subsequently, the sections were re-dyed with eosin Y aqueous solution for 2 min followed by dehydration with graded alcohol and transparent by xylene and sealed with the neutral resin. The prepared slides were examined using a light microscope, and images were captured. Subsequently, the images were imported into ImageJ software, and the lesion area was quantified by manually selecting the region of interest (ROI), which typically consisted of empty vacuoles or other distinct features, and applying a threshold to differentiate the lesion area from the normal tissue. The software then generated the area of the lesion in micrometers.

2.7.2. Immunofluorescence staining

After deep anesthesia, animals were transcardially perfused with PBS followed by 4% paraformaldehyde (PFA) (Sigma, USA). Then, laminectomy was performed to expose the regenerated spinal cord, 1-cm-long spinal cord with a lesion in the center was separated and immersed in 4% PFA at 4 °C overnight followed by 30% sucrose for dehydration. Subsequently, isolated spinal cords were embedded in an optical cutting temperature compound (OCT) (Sakura, USA) and were serial sectioned on a Leica cryostat set at 25 μm thickness. For immunofluorescence staining, sections were firstly washed three times with PBS and then were incubated in the PBS with 10% goat serum (Solarbio, China) and 0.5% Triton X-100 (Sigma, USA) for at least 1 h at room temperature. Then the sections were incubated with diluted primary antibodies against NeuN, Ki67, Casp3, and Iba1 at 4 °C overnight in a humidified container. After three times washes by PBS, sections received the following secondary antibodies (Alexa Fluor 488 and 555) for another 1 h at room temperature. We repeated the washing steps and incubated the sections with DAPI for 5 min, and the sections were finally mounted by fluoromount G (Sigma, USA). These antibodies are highly specific for their targets and have been extensively used in the field. Detailed information on primary and secondary antibodies is listed in Table 1.

2.7.3. Image processing and quantification

The images were captured by confocal microscopy (SP8, Leica, Germany). The densitometry analysis was conducted using ImageJ software (NIH, USA). All experiments were repeated at least 3 times (n = 3) using independent samples. For the lesion area analysis of HE staining, 5–6 random sections of each sample containing the lesion were manually outlined and quantified by ImageJ.

For the quantification of immunofluorescence sections, 5–7 images were chosen for analysis for each sample. Neuron survival, cell proliferation, and apoptosis around the lesion core were calculated. Specifically, the amount of $NeuN^+$, $Ki67^+$, and $Casp3^+$ marked cells was counted within two 600 × 600 μm squares using ImageJ, which was located rostrally and caudally from the lesion area. For inflammatory analysis in the spinal cord, we analyzed the expression of Iba1 (specifically for macrophage and microglia), which was calculated within square areas of 100 × 100 μm, 6 squares both in the direction of head and tail from the lesion center [26].

Table 1
Antibodies and dilutions used for Immunofluorescence staining and Western blot analysis.

	Antigen	Company	Species	Dilution
Primary antibody	NeuN	Abcam, UK, ab279296	Mouse	1:500
	Ki67	CST, USA, 9129S	Rabbit	1:1000
	Casp3	CST, USA, 9661S	Rabbit	1:400
	Iba1	Wako, Japan, 019–19741	Rabbit	1:500
	PI3K	CST, USA, 4228T	Rabbit	1:1000
	β-actin	CST, USA, 4970T	Rabbit	1:1000
Secondary antibody	Alexa 488	Abcam, UK, ab150077	Goat anti-rabbit	1:400
	Alexa 555	Abcam, UK, ab150114	Goat anti-mouse	1:400
	HRP-linked Antibody	Servicebio, China, GB23303	Goat anti-rabbit	1:1000

Table 2
Scores and operational definitions for the Basso Mouse Scale for locomotion (BMS).

Score	
0	No ankle movement
1	Slight ankle movement
2	Extensive ankle movement
3	Plantar placing of the paw with or without weight support –OR Occasional, frequent or consistent dorsal stepping but no plantar stepping
4	Occasional plantar stepping
5	Frequent or consistent plantar stepping, no coordination –OR Frequent or consistent plantar stepping, some coordination, paws rotated at initial contact and lift off (R/R)
6	Frequent or consistent plantar stepping, some coordination, paws parallel at initial contact (P/R, P/P) –OR Frequent or consistent plantar stepping, mostly coordinated, paws rotated at initial contact and lift off (R/R)
7	Frequent or consistent plantar stepping, mostly coordinated, paws parallel at initial contact and rotated at lift off (P/R) –OR Frequent or consistent plantar stepping, mostly coordinated, paws parallel at initial contact and lift off (P/P), and severe trunk instability
8	Frequent or consistent plantar stepping, mostly coordinated, paws parallel at initial contact and lift off (P/P), and mild trunk instability –OR Frequent or consistent plantar stepping, mostly coordinated, paws parallel at initial contact and lift off (P/P), and normal trunk stability and tail down or up & down
9	Frequent or consistent plantar stepping, mostly coordinated, paws parallel at initial contact and lift off (P/P), and normal trunk stability and tail always up

2.8. Electron microscopy examination and analysis

The electron microscopy was conducted on mouse spinal cord sections. Samples of $2 \times 2\ mm^3$ rostrally from the lesion were first subjected to the fixation by 3% glutaraldehyde for at least 2 h, and then incubated in the 1% osmium tetroxide solution for 1.5 h. After well dehydrated, ultrathin transverse sections were made (50 nm thickness) and then examined under the transmission electron microscope (HT7700; Hitachi, Japan).

All the electron microscopy analyses were performed using Image-pro Plus software. Each sample would randomly select 8 fields to measure the density and diameter of myelinated nerve, and the thickness of myelin sheaths. We also calculated the G-ratio, another measure of the thickness of myelin sheaths, using the following formula: $G-\text{ratio} = \frac{\text{the inner diameter}}{\text{the outer diameter}} \times 100\%$ of the myelin.

2.9. Enzyme-linked immunosorbent assay (ELISA) and G-Series Mouse Cytokine Array

1-cm-long spinal cord with a lesion at the center was isolated as aforementioned and lysed by RIPA Lysis buffer and then quantified using the BCA protein assay kit (Beyotime, China). Then, for the measurement of trophic factors of each group, the tissue supernatant was collected for ELISA of BDNF, NGF, NT-3, and VEGF according to the manufacturer's instructions, respectively. As for the measurement of cytokines expression, the same supernatant was measured using the G-Series Mouse Cytokine Array, a semi-quantitative measurement kit of 40 mouse cytokines, according to the manufacturer's protocol.

2.10. RNA sequencing analysis

The RNA sequencing analysis was performed as in our previous study [2]. Briefly, a 1-cm-long spinal cord with the lesion in the center was separated from the mouse at 35d post-injury in the SCIT and SCI group ($n = 3$ in each group) as stated above. Then the total RNA of the 1-cm-long spinal cord was extracted using TRIzol reagents following the manufacturer's protocol. cDNA library was prepared with the RNA Nano 6000 Assay Kit of the Bioanalyzer 2100 system (Agilent Technologies, CA, USA). Then the high-throughput of the cDNA was performed on a cBot Cluster Generation System using TruSeq PE Cluster Kit v3-cBot-HS (Illumia) according to the manufacturer's instructions (from Beijing Novel Bioinformatics Co., Ltd. (https://en.novogene.com/)). The data process and analysis were similar to our previous study. Raw sequencing data with FPKM calculation results are accessible at the GEO database (http://www.ncbi.nlm.nih.gov/geo/) under accession ID GSE 193806.

2.11. Western blot analysis

For the further verification of the PI3K-AKT pathway played in the regeneration process of SCI mice with rotarod training, the Western blot analysis has been applied to the experiment as previously stated [27]. In brief, the protein extracting and quantifying process was similar to the ELISA as stated above. 10 μl primary antibody rabbit anti-PI3K (diluted with TBST at the ratio of 1:1000) was used to detect the PI3K expression, followed by 10 μl alkaline phosphatase-labeled second antibody with similar dilution. The β-actin was selected as the internal control. All procedures were performed according to the manufacturer's instructions. After that, all the gray-scale values were calculated and analyzed by Image J software.

2.12. Statistical analysis

The statistical analysis in this study was performed using SPSS 24.0 (IBM, USA). All quantitative data were expressed as the mean ± standard deviation (SD). Differences between different groups were compared using unpaired Student's t-test or one-way ANOVA

followed by Bonferroni posthoc test for multiple comparisons if data obeyed the normal distribution and had homogeneous variances. Otherwise, a non-parametric test was selected for further analysis. A two-sided Wilcoxon signed-rank test was used for matched data pairs, and the Mann–Whitney *U* test was used for unpaired data. The P value < 0.05 was considered statistically significant.

3. Result

3.1. Rotarod training impaired functional recovery after SCI

To evaluate whether rotarod training could improve functional recovery after SCI, mice were compared using the electrophysiological assessment, Catwalk gait analysis, BMS locomotion test, and rotarod test.

For the electrophysiological evaluation, the amplitude and latency were recorded and compared among the groups (Fig. 1A and B).

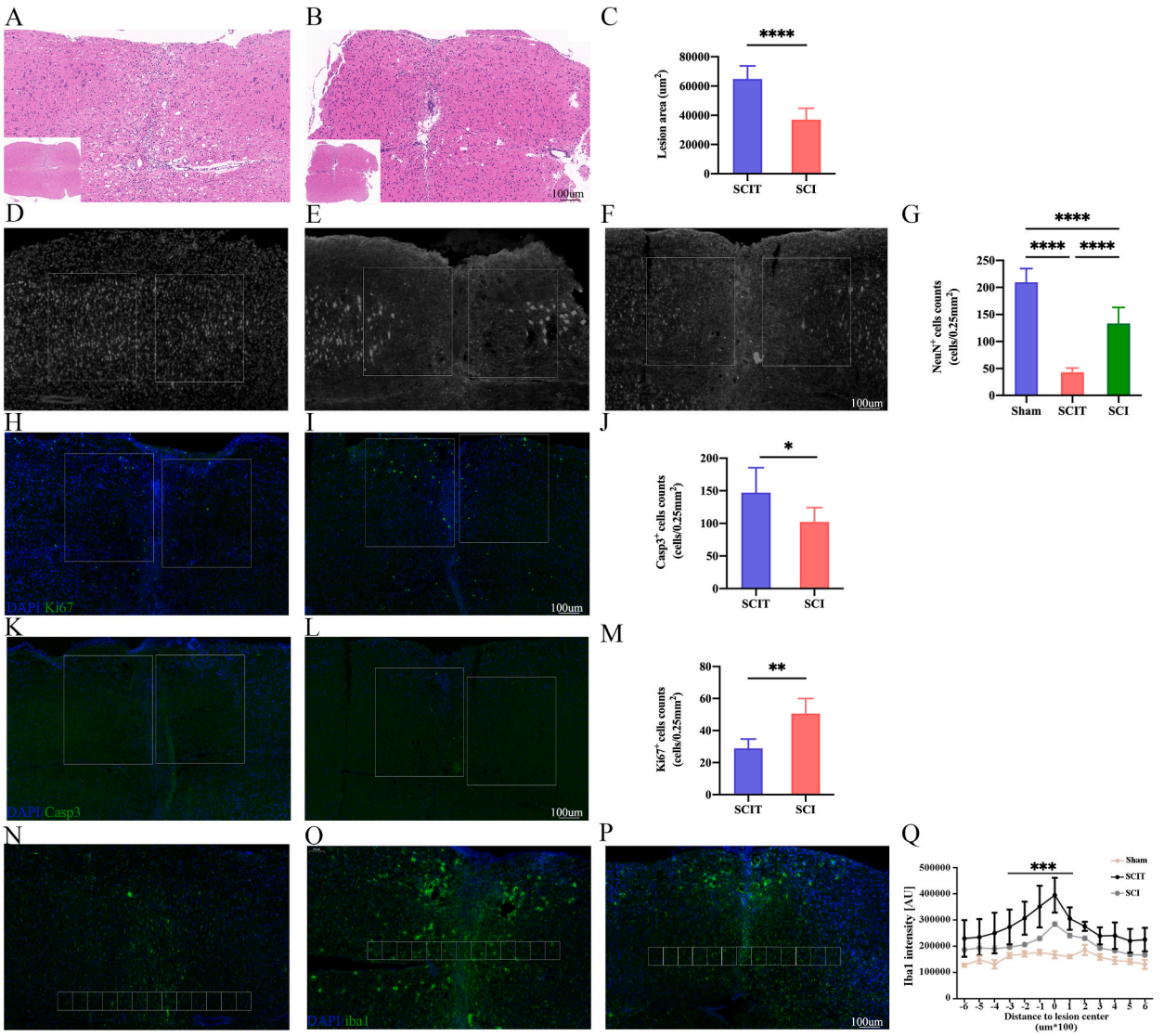

Fig. 2. The histological evaluation of SCIT and SCI groups. **A-C** The HE staining shows the lesion at the center of the spinal cord in SCIT (A), and SCI group (B). The left bottom of A and B showed the full view of the representative sample. The statistical analyses were conducted in C (n = 6 in each group). Scale bar = 100 μm. **D-L** The immunofluorescence staining showed the $NeuN^+$, $Ki67^+$, and $Casp3^+$ cells in SCIT (D, G, J), and SCI group (E, H, K). The number of $NeuN^+$, $Ki67^+$, and $Casp3^+$ cells was calculated within two 600 × 600 μm squares, which were just located rostrally and caudally from the lesion area. The statistical analyses were conducted in (F, I, L, n = 6 in each group). Scale bar = 100 μm. **M-O** The immunofluorescence staining showed inflammation in SCIT (M), and SCI group (N) at 5 weeks post-SCI. Scale bar = 100 μm. The intensity of Iba1 expression was calculated within 100 × 100 μm square areas extending 600 μm both rostrally and caudally from the lesion center. The statistical analyses were conducted in (O). Scale bar = 100 μm. n = 6 mice in each group. *** indicate P < 0.001.

As shown in Fig. 1C and D, injured mice with rotarod training or without rotarod training presented a very small response at 28d post injury (no significant difference was detected between the two groups), while mice in the Sham group (uninjured spinal cord) demonstrated much higher amplitude and shorter latency, indicating that rotarod training made no difference on synapse connections after SCI.

For Catwalk gait analysis, the step sequence, base of support (the sign of trunk stability), and regularity index (the evaluation of coordination) were recorded and analyzed in all three groups. As shown in Fig. 1E–G, the abnormal gait was detected, and the trunk stability and coordination were immediately affected post-injury and exhibited mild if any, spontaneous recovery at 14, 21, and 28d post-injury in both SCIT and SCI groups There was no significant difference in the length of the base of support between mice in SCIT and SCI group at all evaluated time points. Worse still, although mice in the SCIT group showed a similar regularity index with those in the SCI group at T-7d, T-14d, and T-21d, SCIT mice showed a significantly lower regularity index than SCI mice at T-28d. Namely, rotarod training did not improve trunk stability but worsened the coordination in mice after injury.

For the locomotion test, the motor function of the hindlimb was calculated at -7d, 0d, 7d, 14d, and 28d following training according to BMS scoring. As shown in Fig. 1H, all the injured hindlimbs showed immediate paralysis after SCI, whereas mice in the sham group demonstrated no significant functional impairment. Then mice in both SCIT and SCI groups showed functional recovery to varying degrees. In the SCIT group, the BMS score was similar to that of the SCI group after 7d training (T-7d). However, continuous rotarod training gradually impaired mice's functional recovery when compared with the SCI group at T-14d and T-28d.

We also conducted the rotarod test on mice in three groups to evaluate the functional recovery after SCI (Fig. 1J). We found that mice in the SCIT group, not the SCI group stood longer on the rod at 14d, 21d, and 28d post-training, implying a better motor recovery of the SCIT group in the rotarod test (Fig. 1I). This better performance of stablity should be explained with cautions. On the one hand, the mice in the SCIT group were expected to stay on the rod for a long time because they were trained with high intensity. On the other hand, although the rotational motion ability of the SCIT group was better than that of the SCI group, it still decreased significantly

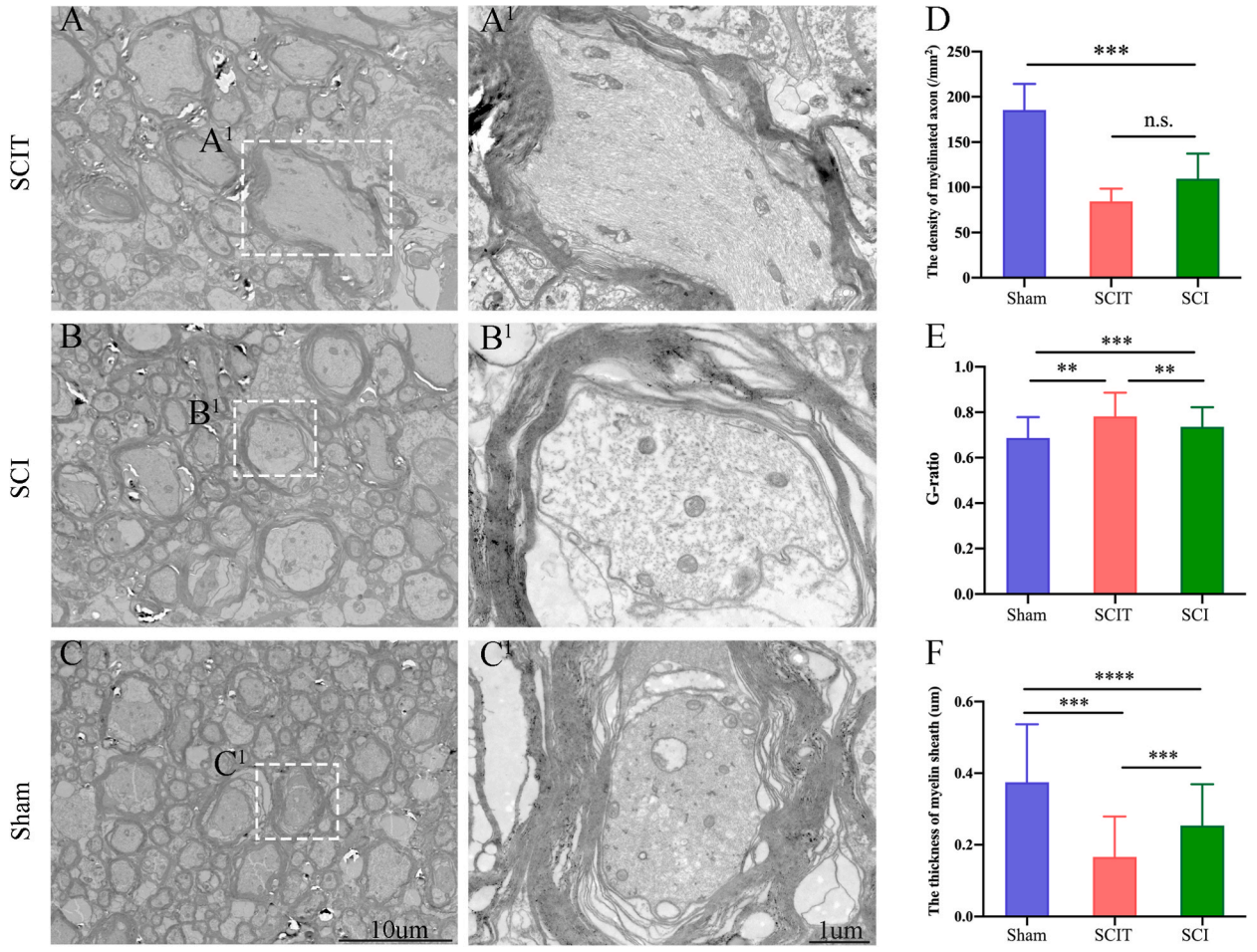

Fig. 3. Nerve remyelination analysis in three groups. **A-C** The representative transmission electron micrographs at 5 weeks post-SCI. Scale bar = 10 μm. **A′-C′** The magnification of the regions of interest in A-C marked by the white square. Scale bar = 1 μm. **D-F** The histograms comparing the density of myelinated axons, G-ratio, and the thickness of myelinated sheath among three groups (n = 6 mice in each group). **, *** and n.s. indicate $P < 0.01$, $P < 0.001$, and no statistical difference, respectively.

compared with that of the sham group. In addition, the differences between the SCIT and SCI groups remained consistent from two weeks after training. Hence, these results implied that rotarod training was unable to promote electrophysiological improvements and trunk stability as expected. On the contrary, it may impair the recovery of functional coordination and locomotion.

3.2. Rotarod training has adverse effects on spinal cord regeneration after SCI

Considering the undesirable effects of rotarod training on functional recovery, we next used histopathology to analyze whether rotatory training could help injured tissue regenerate. The spinal cord hemisection was first performed at the T10 segment, and mice with or without 28d training were euthanatized for further histopathological assessment. Firstly, we evaluated the size of the lesion cavity by HE staining sections. As shown in Fig. 2A–C, compared with the SCI group, the injury area was significantly larger, and more vacuoles were detected in the SCIT group, indicating that rotarod training worsened the lesion profile.

Then we assessed the neuronal viability, cell proliferation, and apoptosis around the lesion core of the spinal cord using NeuN, Ki67, and Casp3 immunofluorescence and analyzed whether rotarod training could rescue the injured neurons and promote cell proliferation. As shown in Fig. 2D-M, the neurons that survived in the SCI group (161 ± 30.9) were significantly less than that of the SCIT group (43.3 ± 7.63). In addition, compared with the SCI group, the number of Ki67^{+} cells was lower and the number of Casp3^{+} cells was higher in mice in the SCIT group after SCI, indicating that rotarod training could deteriorate cell proliferation and induce cell apoptosis in mice after SCI.

We also examined the local immuno-microenvironment by evaluating the activation process of microglia/macrophages via assessing the expression of Iba1, which was a typical hallmark of neuropathy following SCI. As shown in Fig. 2 N-Q, the expression intensity of Iba1 around the injured area in the SCIT group was higher, especially in the area of rostral 300 μm to caudal 100 μm, suggesting that rotarod training could activate microglia/macrophages after SCI.

We further analyzed the role of rotarod training in nerve regeneration, particularly remyelination by analyzing the TEM images of the proximal spinal cord. As shown in Fig. 3, the Sham group exhibited a compact and uniform structure consisting of a clear and dense myelin sheath, while both SCIT and SCI groups showed a sparse and heterogeneous structure of myelin sheath. SCIT group showed a lower density of myelinated axons, higher G-ratio value, and thinner myelin sheath than the SCI group, suggesting that rotarod training

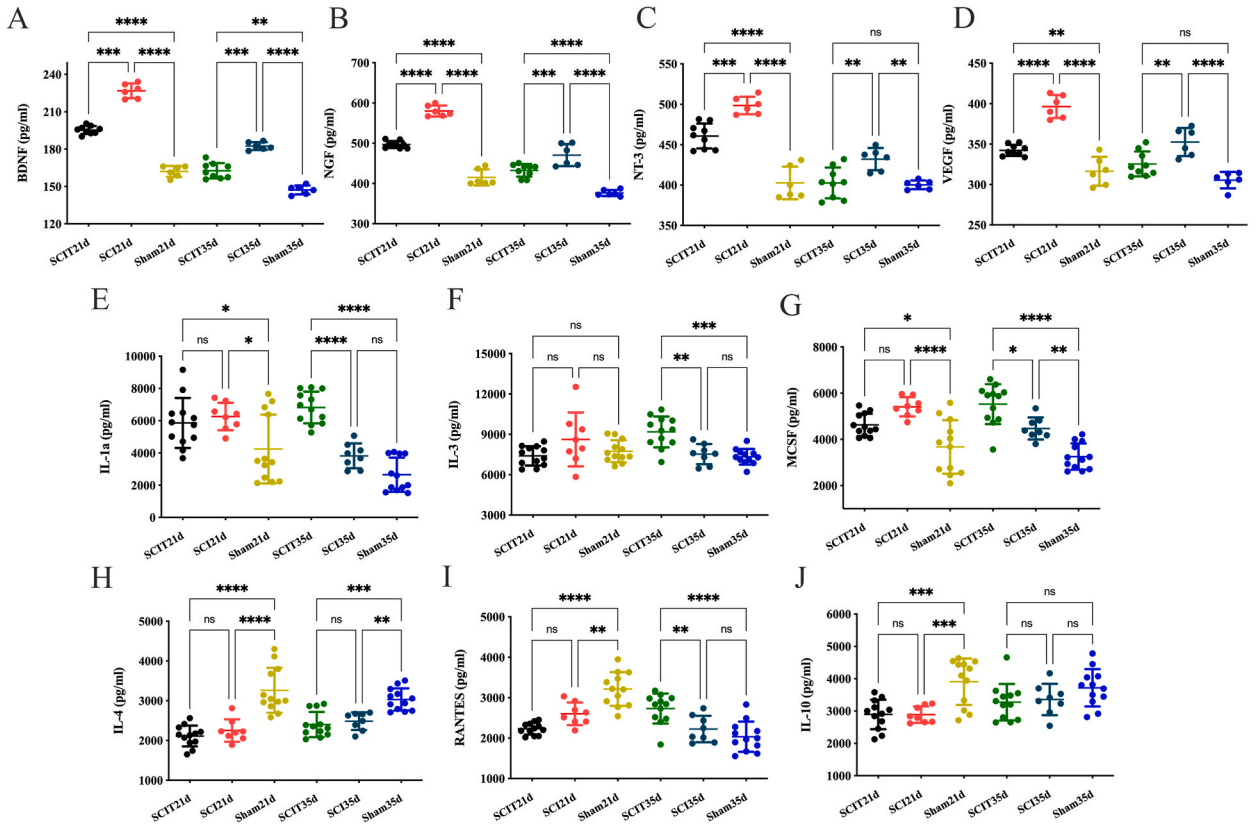

Fig. 4. Expression profile of trophic factors and cytokines. **A-D** The analysis of expression of trophic factor BDNF, NGF, NT-3, and VEGF through ELISA both at 21 days and 35 days after SCI. ***E*-J** The analysis of cytokines expression including pro-inflammatory factors (IL-1a, IL-3, MCSF, and RANTES) and anti-inflammatory factors (IL-4 and IL-10) using the G-Series Mouse Cytokine Array. *, **, *** and n.s. indicate $P < 0.05$, $P < 0.01$, $P < 0.001$, and no statistical difference, respectively.

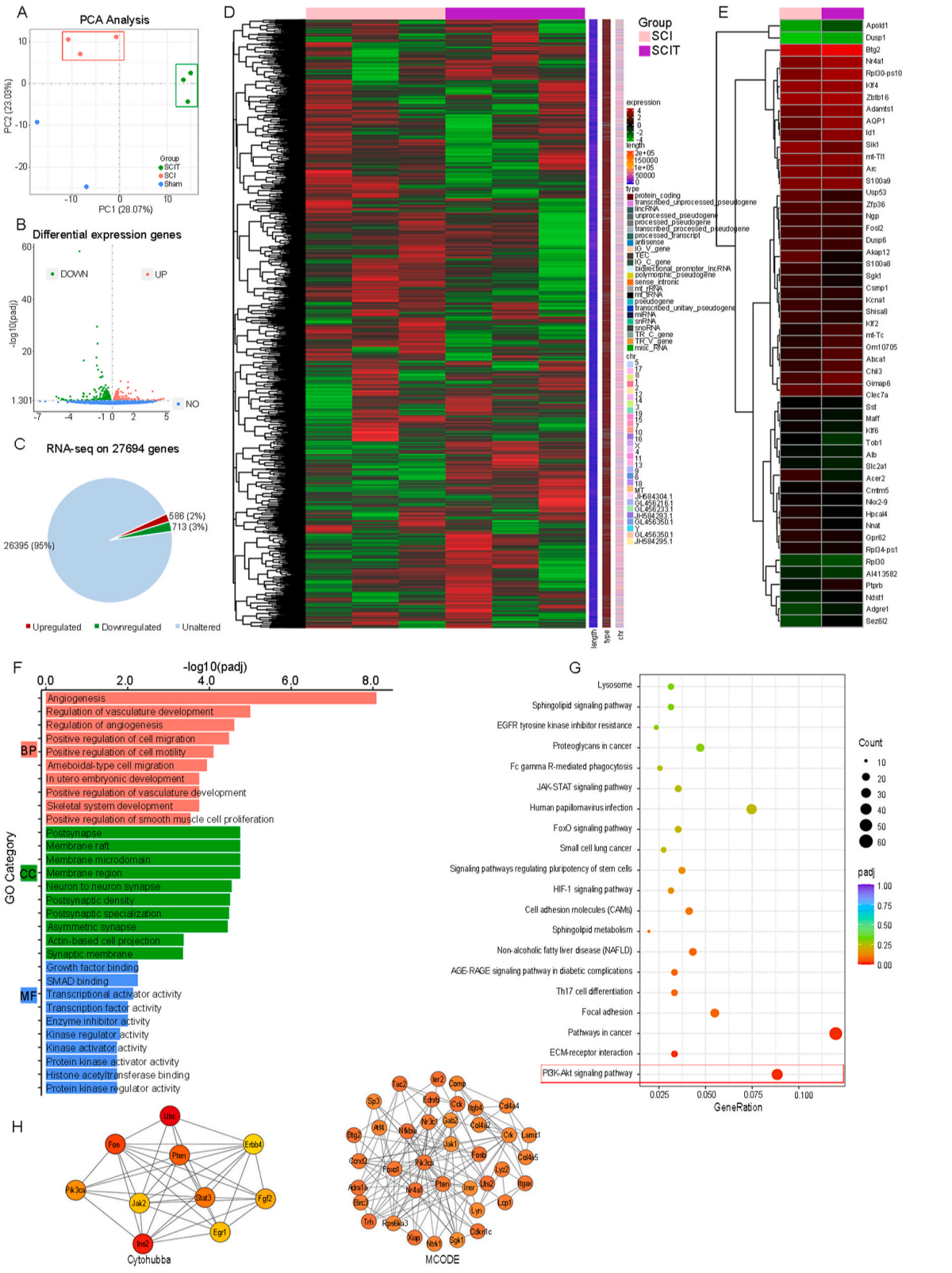

(caption on next page)

Fig. 5. RNA sequencing of gene expression between SCIT and SCI group. **A** The PCA analysis showed gene expression was scattered between groups but clustered within groups. **B** The volcano plot showed the DEGs between SCIT and SCI groups, with red and green denoting the upregulation and downregulation, respectively. **C** Among 27,694 genes, 586 genes were upregulated while 713 genes were downregulated. **D, E** All of the DEGs as well as the top 50 DEGs were displayed in the heatmap with hierarchical clustering analysis. **F** The GO analysis showed the top 10 significantly enriched categories in biological process (BP), cellular component (CC), and molecular function (MF). **G** The KEGG analysis exhibited the top 20 significantly enriched pathways. **H** The protein-protein network and modular analysis (Cytohubba and MCODE) with the representative DEGs like Pten and Pik3ca. (For interpretation of the references to colour in this figure legend, the reader is referred to the Web version of this article.)

was unfavorable to remyelination following SCI.

Therefore, rotarod training exhibited significant negative effects on spinal cord repair in terms of the lesion area, neuronal viability, cell proliferation, apoptosis, immuno-microenvironment, and remyelination.

3.3. Rotarod training played a detrimental role in neuroprotection via inhibiting trophic factors but promoting inflammatory factors secretion

Since rotarod training was detrimental to spinal cord repair, to understand the mechanism of its deterioration, we further explored the expression profile of trophic factors and inflammatory factors, which took an important part in tissue repair. We examined the expression of four trophic factors (BDNF, NGF, NT-3, and VEGF) using an ELISA kit at 21 and 35 days after spinal cord injury (SCI). Our results, shown in Fig. 4A–D, indicate that concentrations of all four trophic factors were significantly reduced in all groups at either 21 or 35 days. Moreover, a statistically significant difference in trophic factor concentrations was observed between the SCI and SCIT groups at both time points.

Specifically, at 21 days after SCI, the concentrations of trophic factors were as follows: BDNF (227 ± 5.89 vs 195 ± 3.20 pg/ml, $P < 0.001$), NGF (580 ± 13.6 vs 497 ± 8.75 pg/ml, $P < 0.001$), NT-3 (499 ± 10.8 vs 461 ± 15.5 pg/ml, $P < 0.001$), and VEGF (396 ± 14.2 vs 342 ± 6.82 pg/ml, $P < 0.001$). Similarly, at 35 days after SCI, the concentrations of trophic factors were as follows: BDNF (183 ± 3.13 vs 163 ± 6.17 pg/ml, $P < 0.001$), NGF (471 ± 27.3 vs 433 ± 15.7 pg/ml, $P < 0.001$), NT-3 (432 ± 13.8 vs 403 ± 19.1 pg/ml, $P < 0.001$), and VEGF (353 ± 17.3 vs 325 ± 15.4 pg/ml, $P < 0.001$).

For inflammatory factors, we applied the G-series Mouse Cytokine Array to assess cytokine secretion. As shown in Fig. 4E–J, there was no significant difference between the SCIT and SCI group 21d after injury. However, at 35d after injury, the SCIT group suppressed the expression of pro-inflammatory factors (IL-1a, IL-3, MCSF, and RANTES), but did not affect the secretion of typical anti-inflammatory factors (IL-4 and IL-10).

Thus, these results suggested that rotarod training leads to a significant reduction in trophic factors and an increase in the expression of some specific pro-inflammatory factors, which is detrimental to neuroprotection after SCI.

3.4. RNA-seq analysis of rotarod training on SCI

To determine the potential mechanisms of rotarod training's adverse effects on functional recovery, cytokines secretion, and tissue protection and repair, we then performed high-throughput RNA sequencing for three groups. Sup. Table 1 presented the quality control results of RNA-seq and guaranteed the data's reliability.

As shown in Fig. 5A, the sample's gene expression between SCIT and SCI groups was visibly scattered, whereas the gene expression within groups was clustered together via PCA analysis, inferring that the SCIT group has a distinct gene profile from the SCI group. The further analysis of differential expression gene (DEG) demonstrated that there were 1299 DEGs between two groups with 586 upregulated genes and 713 downregulated genes (Fig. 5B and C). All the DEGs were displayed in the hierarchical clustering heatmap (Fig. 5D), and the top fifty DEGs were shown in Fig. 5E, and summarized in Sup. Tables S2 and S3. Moreover, GO enrichment analysis revealed that DEGs, especially the down-regulated genes, were primarily associated with the re-vascularization biological process like angiogenesis, regulation of vasculature development, regulation of angiogenesis, and cellular component including post-synapse, neuron-to-neuron synapse, etc. (Fig. 5F and Sup. Table S4). On the other hand, KEGG pathway analysis showed that those significantly altered genes, also down-regulated DEGs in particular, were mainly enriched in the PI3K-Akt signaling pathway (Fig. 5G and Sup. Table S5).

To explore the interactive relationships among the DEGs here, we used the protein-protein interaction network (PPI) and modular analysis (Cytohubba and MCODE) to determine the functional gene clusters. As expected, we found that the main function modules were associated with the PI3K-Akt signaling pathway, be it the Cytohubba or the MCODE app, and the representative DEGs like Pten and Pik3ca might play a major role in the aforementioned process. To further verify the roles of PI3K-Akt pathway played in the effects of rotarod training on SCI, we measured the protein expression of PI3K via Western blot analysis (Sup. Fig. 2). It showed that PI3K expression was significantly inhibited in the SCIT group when compared with that in the SCI group, which was similar to our RNA-sequencing results.

Taken together, these data implied that the inferior effects of rotarod training on SCI could be attributed to the inhibition of the angiogenesis process, synapse formation, and the inactivation of the PI3K-Akt signaling pathway.

4. Discussion

Previous research has shown that the rehabilitative exercise, be it a single task or combined tasks, might promote functional

recovery following SCI [5,28–30].

Non-invasive interventions, including various types of locomotor training (e.g., ladder walking, reaching, bicycling, swimming, and training on a treadmill) decrease the inflammatory response, increase neurotrophin levels, and may strengthen spared functions, and guide spinal reorganization. Locomotor training successfully improves the recovery of stepping movements in various animal models. However, locomotion training might also have worsening outcomes. It is necessary to continuously acquire new insights into the effective rehabilitative training modality, which could promote determining which kinds of training should be considered for further clinical practice.

In this study, we, for the first time, assessed the effects of rotarod training for 4 weeks on the spinal cord repair and functional recovery of mice with SCI in terms of electrophysiology, gait analysis, BMS score, and histological and cellular function assessment. Unexpectedly, we discovered that 4-week-long rotarod training could not improve the electrophysiological activities and step stability of SCI mice, but impaired the functional recovery of coordination and locomotion after SCI. Mice in the SCIT group did not show better recovery on any tests except the rotarod test. On the whole, our results showed that rotarod training played negative roles in spinal cord repair concerning lesion size, neuronal viability, cell proliferation, apoptosis, immuno-microenvironment, and remyelination. Even worse, we observed that mice in the SCIT group experienced a significant reduction of trophic factors and increased pro-inflammatory factors expression, which were detrimental to tissue repair following SCI. Our study indicated that immediate rotarod training after SCI had very limited effects on functional recovery, and the timing of rotarod training might affect the repair of spinal cord injury.

To explore the potential mechanism of rotarod training's limited effects on functional recovery in our study, further investigation was applied to figure out the molecular mechanisms underlying the differences between SCIT and SCI groups. Our results showed that rotarod training significantly changed the gene expression profile of mice. Specifically, the genes associated with angiogenesis and synaptogenesis were down-regulated, which took important parts in the neuroprotection and spinal cord repair. These were consistent with the lower secretion of trophic factors. Also, the expression of genes enriched in the pathway of PI3K-AKT in the SCIT group was inhibited. PI3K-AKT pathway, which is involved in glial scar formation could regulate the strong inflammation and promote functional recovery after SCI [31,32]. This might explain the overwhelming inflammatory response and higher cell apoptosis showed in the SCIT group.

Rotarod training, known as both active-passive rehabilitative exercise, was reported to be an effective neurorehabilitation for CNS injuries [17,19,33,34]. Originally, the rotarod task was created for functional evaluation in neurological disorders or injuries instead of motor training. Unlike other rehabilitative training, rotarod training was increasingly preferred as a training method after neurological disorders due to its overwhelming improvement in the locomotive rhythm, balance, and coordination on objects at the same time [17]. Besides, a previous study indeed showed that rotarod training was able to enhance the functional recovery of limb locomotion after stroke [35] and traumatic brain injury [17].

Several reasons might be responsible for the limited effects of rotarod training in our research. (1) The reason for the deviation may be related to the modeling method. Unlike a stroke or brain injury, the hemisection of the spinal cord directly cut off the bridge of sensorimotor signals input and output in the injured lateral [36,37], which might weaken the therapeutic effects of rotarod training on spinal cord repair; (2) another possible contributing factor might be the substantial spontaneous recovery of the untrained mice. Many studies have stated before that mouse with incomplete SCI would experience spontaneous functional recovery to varying degrees [38–41]. Therefore, the spontaneous recovery of untrained mice might obscure the authentic effects of rotarod training; (3) the lack of enough training periods could also play an important role in counteracting the positive effects of rotarod training. Some of the previous studies have claimed that the long-term training duration (>2 months) was more likely to achieve a meaningful recovery after SCI [10, 42], although the training duration itself was still a matter of some debate; (4) in addition, the intensity of training or the starting time of training might also be important reasons for the aforementioned problem [43,44]. The overexpression of phosphatase and tensin homolog deleted on chromosome 10 (PTEN), key signaling components in the PI3K-akt pathway, could improve axon regeneration at the injury site. One study found that activation of the PI3K/Akt/mTOR pathway in astrocytes 3 days after SCI may be associated with glial scar formation. Because delayed treatment with Ad-PTEN after SCI enhanced motor function recovery more significantly than immediate treatment with Ad-PTEN, the results suggest that the optimal strategy for attenuating glial scar formation may be introduced 3 days after SCI. Therefore, the immediate locomotor therapy after injury may be harmful for tissue repair, but whether introducing locomotor training at least 3 days after injury is worth exploring. Thus, researchers in this field should consider these aspects in the future.

It should be noted that two main limitations exist in our study. First, as there is a rare study on rotarod training after SCI, the training protocol of rotarod training was referred from the studies on brain injuries or stroke. The rehabilitative protocol might need some modifications to boost the therapeutic effect on mice with SCI. Second, to better detect the superiorities of rotarod training in the treatment of SCI, we may need to compare the rotarod training with other classical regimens like treadmill training, which is lacking in our current study.

5. Conclusion

To our knowledge, this study might be the first attempt to explore the effects of rotarod training on locomotion recovery and its potential mechanism for spinal cord repair after SCI. After a series of assessments of rotarod training on SCI in terms of the function evaluation, histopathological characteristics, molecular behaviors, and the profile of specific genes expression, we found that rotarod training aggravated injury and impaired functional recovery after SCI, manifesting bigger lesion area, poorer neuronal viability, worse immuno-microenvironment and remyelination, and significant reduction of trophic factors but increased pro-inflammatory factors

expression. Further RNA sequencing suggested that rotarod training might inhibit the PI3K-AKT pathway and downregulated genes associated with angiogenesis and synaptogenesis, indicating that the current protocol of rotarod training is not suitable for rehabilitation for mice with SCI.

Author contribution

Junhao Deng: Conceived and designed the experiments; Performed the experiments; Analyzed and interpreted the data; Wrote the paper. Fanqi Meng: Performed the experiments; Analyzed and interpreted the data; Wrote the paper. Jianpeng Gao, Kexue Zhang: Performed the experiments. Zhongyang Liu, Ming Li: Analyzed and interpreted the data. Jiantao Li, Yu Wang, Xiao Liu: Contributed reagents, materials, analysis tools or data. Licheng Zhang, Peifu Tang: Conceived and designed the experiments.

Financial support

This research is supported by the Training Program of the Foundation for the Distinguished Young Scholars of PLA General Hospital of China (No. 2020-JQPY-003 to LCZ), the Training Program of the Foundation for the Distinguished Young Scholars of Chinese PLA General Hospital projects (No. 2020-JQPY-003 to LCZ). The Fund's name is Youth Innovation Science Fundation of PLA General Hospital of China (No. 2022QNFC012 to JHD), the National Natural Science Foundation of China (No. 82101435 to KXZ), and the National Natural Science Foundation of China (No. 82272478 to PFT).

Copyright license agreement

The Copyright License Agreement has been signed by all authors before publication.

Data sharing statement

Datasets analyzed during the current study are available from the corresponding author upon reasonable request.

Data availability statement

Data associated with this study has been deposited at GEO database (http://www.ncbi.nlm.nih.gov/geo/) under the accession number GSE 193806.

Declaration of competing interest

The authors declare that they have no known competing financial interests or personal relationships that could have appeared to influence the work reported in this paper.

Sup. Fig. 1 The graphic abstract of the rotarod training on spinal cord injury.

Sup. Fig. 2 The Western blot analysis of PI3K expression between SCIT and SCI groups. A The protein expression of PI3K (upper panel) and the internal control β-actin (bottom panel) were tested by the Western blot. B The relative PI3K expression was significantly lower in the SCIT group than in the SCI group (n = 2 in each group, and the Western blot test had been performed twice). * indicates P < 0.05.

Sup. Table 1 Quality control summary of the RNA sequence results of three groups.

Sup. Table 2 List of the top 50 upregulated genes following acute rotarod training.

Sup. table. S3 List of the top 50 downregulated genes following **acute rotarod training.**

Sup**. table. S4 List of the top 50 GO terms following acute rotarod training.**

Sup. table. S5 List of the top 20 terms of KEGG pathway following **acute rotarod training.**

Acknowledgements

We appreciated the instructions and help from the Orthopedics Institute of Chinese PLA for providing the necessary experimental facilities for this study.

Appendix A. Supplementary data

Supplementary data related to this article can be found at https://doi.org/10.1016/j.heliyon.2023.e18158.

References

[1] P. Assinck, G.J. Duncan, B.J. Hilton, J.R. Plemel, W. Tetzlaff, Cell transplantation therapy for spinal cord injury, Nat. Neurosci. 20 (2017) 637–647.
[2] J. Deng, M. Li, F. Meng, et al., 3D spheroids of human placenta-derived mesenchymal stem cells attenuate spinal cord injury in mice, Cell Death Dis. 12 (2021) 1096.
[3] J. Deng, Y. Zhang, Y. Xie, L. Zhang, P. Tang, Cell transplantation for spinal cord injury: tumorigenicity of induced pluripotent stem cell-derived neural stem/progenitor cells, Stem Cell. Int. 2018 (2018), 5653787.
[4] T.H. Hutson, S. Di Giovanni, The translational landscape in spinal cord injury: focus on neuroplasticity and regeneration, Nat. Rev. Neurol. 15 (2019) 732–745.
[5] S. Cobianchi, A. Arbat-Plana, V.M. Lopez-Alvarez, X. Navarro, Neuroprotective effects of exercise treatments after injury: the dual role of neurotrophic factors, Curr. Neuropharmacol. 15 (2017) 495–518.
[6] G. Brazg, M. Fahey, C.L. Holleran, et al., Effects of training intensity on locomotor performance in individuals with chronic spinal cord injury: a randomized crossover study, Neurorehabilitation Neural Repair 31 (2017) 944–954.
[7] R. Sachdeva, C.C. Theisen, V. Ninan, J.L. Twiss, J.D. Houlé, Exercise dependent increase in axon regeneration into peripheral nerve grafts by propriospinal but not sensory neurons after spinal cord injury is associated with modulation of regeneration-associated genes, Exp. Neurol. 276 (2016) 72–82.
[8] C.R. Battistuzzo, R.J. Callister, R. Callister, M.P. Galea, A systematic review of exercise training to promote locomotor recovery in animal models of spinal cord injury, J. Neurotrauma 29 (2012) 1600–1613.
[9] M. Martinez, H. Delivet-Mongrain, H. Leblond, S. Rossignol, Effect of locomotor training in completely spinalized cats previously submitted to a spinal hemisection, J. Neurosci. 32 (2012) 10961–10970.
[10] C.R. Battistuzzo, M.M. Rank, J.R. Flynn, et al., Gait recovery following spinal cord injury in mice: limited effect of treadmill training, The journal of spinal cord medicine 39 (2016) 335–343.
[11] K. Fouad, G.A.S. Metz, D. Merkler, V. Dietz, M.E. Schwab, Treadmill training in incomplete spinal cord injured rats, Behav. Brain Res. 115 (2000) 107–113.
[12] C. Heng, R.D. de Leon, Treadmill training enhances the recovery of normal stepping patterns in spinal cord contused rats, Exp. Neurol. 216 (2009) 139–147.
[13] H.Y. Shin, H. Kim, M.J. Kwon, et al., Molecular and cellular changes in the lumbar spinal cord following thoracic injury: regulation by treadmill locomotor training, PLoS One 9 (2014), e88215.
[14] J.F. Yang, K.E. Musselman, D. Livingstone, et al., Repetitive mass practice or focused precise practice for retraining walking after incomplete spinal cord injury? A pilot randomized clinical trial, Neurorehabilitation Neural Repair 28 (2014) 314–324.
[15] M. Martinez, H. Delivet-Mongrain, S. Rossignol, Treadmill training promotes spinal changes leading to locomotor recovery after partial spinal cord injury in cats, J. Neurophysiol. 109 (2013) 2909–2922.
[16] B.K. Hillen, J.J. Abbas, R. Jung, Accelerating locomotor recovery after incomplete spinal injury, Ann. N. Y. Acad. Sci. 1279 (2013) 164–174.
[17] H. Nakagawa, M. Ueno, T. Itokazu, T. Yamashita, Bilateral movement training promotes axonal remodeling of the corticospinal tract and recovery of motor function following traumatic brain injury in mice, Cell Death Dis. 4 (2013) e534.
[18] M. Buitrago, Short and long-term motor skill learning in an accelerated rotarod training paradigm, Neurobiol. Learn. Mem. 81 (2004) 211–216.
[19] J. Cendelin, I. Korelusová, F. Vozeh, The effect of repeated rotarod training on motor skills and spatial learning ability in Lurcher mutant mice, Behav. Brain Res. 189 (2008) 65–74.
[20] A. Ghosh, F. Haiss, E. Sydekum, et al., Rewiring of hindlimb corticospinal neurons after spinal cord injury, Nat. Neurosci. 13 (2010) 97–104.
[21] D.M. Basso, L.C. Fisher, A.J. Anderson, L.B. Jakeman, D.M. McTigue, P.G. Popovich, Basso Mouse Scale for locomotion detects differences in recovery after spinal cord injury in five common mouse strains, J. Neurotrauma 23 (2006) 635–659.
[22] J. Wang, Y.Q. Zhu, Y. Wang, et al., A novel tissue engineered nerve graft constructed with autologous vein and nerve microtissue repairs a long-segment sciatic nerve defect, Neural Regen Res 16 (2021) 143–149.
[23] H. Cheng, S. Almstrom, L. Gimenez-Llort, et al., Gait analysis of adult paraplegic rats after spinal cord repair, Exp. Neurol. 148 (1997) 544–557.
[24] P. Lu, Y. Wang, L. Graham, et al., Long-distance growth and connectivity of neural stem cells after severe spinal cord injury, Cell 150 (2012) 1264–1273.
[25] Z. Zou, X. Hu, T. Luo, et al., Naturally-occurring spinosyn A and its derivatives function as argininosuccinate synthase activator and tumor inhibitor, Nat. Commun. 12 (2021) 2263.
[26] D. Dooley, E. Lemmens, T. Vangansewinkel, et al., Cell-based delivery of interleukin-13 directs alternative activation of macrophages resulting in improved functional outcome after spinal cord injury, Stem Cell Rep. 7 (2016) 1099–1115.
[27] Z. Jiang, Y. Zhang, X. Chen, et al., microRNA-1271 impedes the development of prostate cancer by downregulating PES1 and upregulating ERbeta, J. Transl. Med. 18 (2020) 209.
[28] M.R. Marques, F.C. Nicola, E.F. Sanches, et al., Locomotor training promotes time-dependent functional recovery after experimental spinal cord contusion, Neuroscience 392 (2018) 258–269.
[29] C.A. Angeli, M. Boakye, R.A. Morton, et al., Recovery of over-ground walking after chronic motor complete spinal cord injury, N. Engl. J. Med. 379 (2018) 1244–1250.
[30] P.J. Ward, A.N. Herrity, S.J. Harkema, C.H. Hubscher, Training-Induced functional gains following SCI, Neural Plast. 2016 (2016) 1–12.
[31] S. Xu, J. Wang, J. Zhong, et al., CD73 alleviates GSDMD-mediated microglia pyroptosis in spinal cord injury through PI3K/AKT/Foxo1 signaling, Clin. Transl. Med. 11 (2021) e269.
[32] S. Xu, J. Wang, J. Jiang, et al., TLR4 promotes microglial pyroptosis via lncRNA-F630028O10Rik by activating PI3K/AKT pathway after spinal cord injury, Cell Death Dis. 11 (2020) 693.
[33] A.R. Luft, S. McCombe-Waller, J. Whitall, et al., Repetitive bilateral arm training and motor cortex activation in chronic stroke: a randomized controlled trial, JAMA 292 (2004) 1853–1861.
[34] C.M. Stinear, P.A. Barber, J.P. Coxon, M.K. Fleming, W.D. Byblow, Priming the motor system enhances the effects of upper limb therapy in chronic stroke, Brain 131 (2008) 1381–1390.
[35] Y. Ding, J. Li, Q. Lai, et al., Motor balance and coordination training enhances functional outcome in rat with transient middle cerebral artery occlusion, Neuroscience 123 (2004) 667–674.
[36] L. Zhang, X. Zhuang, Y. Chen, H. Xia, Intravenous transplantation of olfactory bulb ensheathing cells for a spinal cord hemisection injury rat model, Cell Transplant. 28 (2019) 1585–1602.
[37] H.M. Gransee, W.Z. Zhan, G.C. Sieck, C.B. Mantilla, Localized delivery of brain-derived neurotrophic factor-expressing mesenchymal stem cells enhances functional recovery following cervical spinal cord injury, J. Neurotrauma 32 (2015) 185–193.
[38] J. Kjell, K. Sandor, A. Josephson, C.I. Svensson, M.B. Abrams, Rat substrains differ in the magnitude of spontaneous locomotor recovery and in the development of mechanical hypersensitivity after experimental spinal cord injury, J. Neurotrauma 30 (2013) 1805–1811.
[39] P.K. Shah, G. Garcia-Alias, J. Choe, et al., Use of quadrupedal step training to re-engage spinal interneuronal networks and improve locomotor function after spinal cord injury, Brain 136 (2013) 3362–3377.
[40] F.M. Bareyre, M. Kerschensteiner, O. Raineteau, T.C. Mettenleiter, O. Weinmann, M.E. Schwab, The injured spinal cord spontaneously forms a new intraspinal circuit in adult rats, Nat. Neurosci. 7 (2004) 269–277.
[41] R. Shechter, A. London, C. Varol, et al., Infiltrating blood-derived macrophages are vital cells playing an anti-inflammatory role in recovery from spinal cord injury in mice, PLoS Med. 6 (2009), e1000113.

[42] H. Wang, N. Liu, Y.P. Zhang, et al., Treadmill training induced lumbar motoneuron dendritic plasticity and behavior recovery in adult rats after a thoracic contusive spinal cord injury, Exp. Neurol. 271 (2015) 368–378.
[43] C.R. Battistuzzo, R.J. Callister, R. Callister, M.P. Galea, A systematic review of exercise training to promote locomotor recovery in animal models of spinal cord injury, J. Neurotrauma 29 (2012) 1600–1613.
[44] C.M. Tse, A.E. Chisholm, T. Lam, J.J. Eng, A systematic review of the effectiveness of task-specific rehabilitation interventions for improving independent sitting and standing function in spinal cord injury, J Spinal Cord Med 41 (2018) 254–266.